Journal of Engineering Physics and Thermophysics, Vol. 75, No. 5, 2002

HEAT TRANSFER FOR VERTICAL SURFACES WITH DISCRETE FINS IN THE CASE OF FREE CONVECTION

V. G. Gorobets

UDC 536.245

A mathematical model of heat transfer has been developed and numerical calculations for a vertical surface with discrete fins arranged in staggered order have been carried out. The model accounts for the influence of the heat-conduction properties of the finning material and of the fin size on the conditions of heat transfer. A comparison of the results obtained with the existing numerical and experimental data has been made. This comparison shows that the discretization intensifies the heat-transfer process by 50–70%, and neglect of the heat-conduction properties of the fins leads to overstated values of the removed heat fluxes.

One of the known methods of intensifying heat exchange on developed heat-exchange surfaces is the use of finning with a periodic separation of the boundary layer at the initial stages of its formation where the local heat-transfer coefficients are maximum. Such intensification is attained with the use of discontinuous finning with fins of small size in the direction of the flow, which makes it possible to intensify the heat transfer of the finned surfaces by a factor of 1.5–2 in comparison with surfaces having a continuous finning [1, 2]. Nevertheless, theoretical and experimental investigations of surfaces with a discrete finning for the conditions of forced and natural convection are few and ignore a number of factors important for designing specific heat-exchange devices. In particular, for heat exchangers operating under free-convection conditions (air heaters, cooling devices of radioelectronic equipment, heat accumulators, and others) it is necessary to take into account the heat-conduction properties of the material from which the fins are manufactured and their size. For example, the experimental investigation [3] has shown that neglect of the heat-conduction properties of the material from which the finned surface is manufactured leads to an overstated heat-exchange intensification calculated for isothermic surfaces [4]. Taking account of the heat-conduction properties is important in selecting the finning size; this being so, it is of interest to develop the methods for calculating discretely finned surfaces of finite conductivity. Below we develop a mathematical model and conduct numerical calculations for vertical surfaces with a discrete finning arranged in staggered order for the conditions of free-convection heat exchange.

Let us consider a vertical surface with a discrete finning (Fig. 1). Assuming that the thickness of the fins is small ($\delta_f << s$) and ignoring the influence of the last rows of fins, we may separate an elementary portion of this system of width $s' = s/2$ (Fig. 2). Then we analyze the conditions of flow and heat exchange on the separated portion of the heat-exchange surface. On the lower plate or on fin 1 (numbering of the fins is made for two neighboring rows, beginning with the lower one), the boundary layer is formed due to the free-convection flow of the external heat-transfer agent (Fig. 2). In the region of the trailing edge, the boundary layer is separated from the surface and above the plate we have cocurrent flow (facula) which reaches the plate located higher (fin 3). A boundary layer characteristic of mixed-convection flows is formed on the surface of plate 3. The profile of velocities and temperatures in this boundary layer is formed under the action of two factors: (1) the flow due to the heating of the heat-transfer agent on the surface of the plate and (2) the external forced cocurrent flow. The flow behind plate 3 develops as a result of the interaction of the facula from plate 1 and the wake behind plate 3. We note that at a short distance from the separation the characteristics of the cocurrent flow depend no longer on the geometric and thermophysical properties of the heat sources, and the determining factor is the heat power released by these sources. The mechanism of formation of the boundary layer on plate 5 is similar to that on plate 3.

Upon coalescence of the cocurrent flows, the velocity profile is equalized in the neighboring rows in the interfin space and it may be considered to a first approximation as being constant in the cross section. In this case, the

Institute of Technical Thermal Physics, National Academy of Sciences of Ukraine, Kiev, Ukraine. Translated from Inzhenerno-Fizicheskii Zhurnal, Vol. 75, No. 5, pp. 100–107, September–October, 2002. Original article submitted November 26, 2001.

 1062-0125/02/7505-1130$27.00

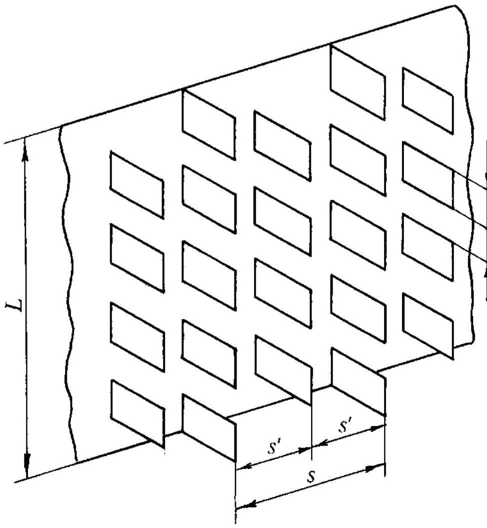

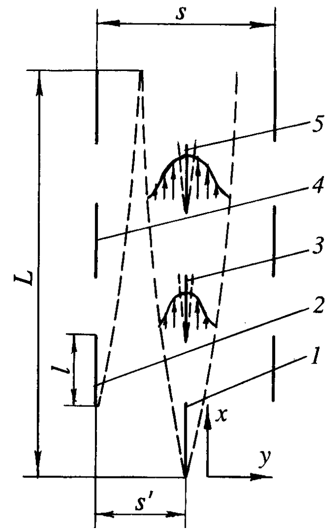

Fig.1. Diagram of the surface with discrete fins.

Fig. 2. Diagram of flow in the interfin channel [1–5) numbering of fins].

velocity changes along the height of the interfin channel. Starting from the analysis of the hydrodynamics and heat exchange in the interfin channel, we develop a mathematical model of the heat-transfer process for the separated portion of the finned surface (Fig. 2).

In thermally thin fins ($\mathrm{Bi_f} = \overline{\alpha}\delta_f/\lambda_f << 1$) for which the condition $l << h$ is fulfilled, the heat transfer is described by the equation

$$\frac{\partial^2 \theta_i}{\partial Z^2} = \frac{2h^2}{\lambda_f \delta_f} q_i\,(\theta_i, X, Z)/(T_0 - T_{g\infty})\,, \quad i = 1, 2, ..., n\,. \tag{1}$$

On condition that the heat loss from the face is neglected, the corresponding boundary conditions have the form

$$\theta_i\,(Z = 0) = 1\,, \quad \left.\frac{\partial \theta_i}{\partial Z}\right|_{Z=1} = 0\,, \tag{2}$$

where i is the number of the fin. The values of the local heat fluxes $q_i(\theta_i, X, Z)$ removed from the surface of the ith fin depend on the conditions of flow and heat exchange. Let us consider these conditions. For fin 1, the density of the removed heat flux is determined by the expression

$$q_1\,(\theta_1, Z) = \overline{\alpha}_1\,(Z)\,(T_1 - T_{g\infty})\,. \tag{3}$$

The heat-transfer coefficient averaged over the width of the fin $\overline{\alpha}_1 = \mathrm{Nu}_l \lambda_g / l$ is found from the formula [5]

$$\mathrm{Nu}_l\,(x) = c\,(\mathrm{Pr})\,\mathrm{Gr}_l^{1/4}\,, \tag{4}$$

where the parameter $c(\mathrm{Pr})$ has the following form:

$$c\,(\mathrm{Pr}) = \left(\frac{\mathrm{Pr}}{2.435 + 4.884\,\mathrm{Pr}^{1/2} + 4.953\,\mathrm{Pr}}\right)^{1/4}. \tag{5}$$

In the region of the wake immediately behind fin 1, the velocity and temperature profiles are complex in character [5]. However, as has been noted above, at small distances from the trailing edge of the plate, the flow in the region of the wake has all the indications characteristic of the faculae from linear heat sources and is independent of the geometry of the source [5]. In this case, because of the small width of the fins it may be assumed that the line of the point source is coincident with the axis line of the fin and has a coordinate $x_1 = l/2$. To calculate the cocurrent flow from the linear heat source, we assume that the cocurrent flow is self-similar and use the solutions presented in [6]. In this case, the longitudinal component of the flow velocity, the temperature of the heat-transfer agent on the axial line, and the thickness of the boundary layer for the cocurrent flow are equal to

$$U_{1x} = \left(\frac{2g\beta Q_1(Z)}{c_p I}\right)^{2/5} \left(\frac{x - l/2}{\mu\rho}\right)^{1/5} f_N'(\eta = 0)\,, \tag{6}$$

$$T_{g1} - T_{g\infty} = \left(\frac{Q_1^4}{64 g\beta\rho^2\mu^2 c_p^4 I^4}\right)^{1/5} (x - l/2)^{-3/5}\,, \tag{7}$$

$$\delta_{g1} = \left(\frac{16\mu c_p I \nu^2}{g\beta Q_1}\right)^{1/5} \eta_e\,(x - l/2)^{2/5}\,, \tag{8}$$

where f_N' is the derivative for the self-similar variable $f_N(\eta)$; the velocity of the flow $U_x = \partial\psi/\partial y$ is determined in terms of the stream function $\psi = 4\nu \sqrt[4]{\mathrm{Gr}_x/4}\, f_N(\eta)$, η_e is the value of the self-similar variable $\eta = \frac{y}{x}\sqrt[4]{\mathrm{Gr}_x/4}$ at the boundary of the boundary layer for the cocurrent flow; $I = \int_{-\infty}^{\infty} f'(\eta)\theta_g(\eta)d\eta$, $\theta_g = (T_g - T_{g\infty})/(T_{g1} - T_{g\infty})$; $T_{g1} = T_g(y = 0)$ is the temperature on the axial line of the cocurrent flow [6].

The power of the linear heat source representing fin 1 is equal to

$$Q_1(Z) = 2q_1(Z, T_1)\, l\,. \tag{9}$$

Fin 3 is in the cocurrent flow from fin 1, and the density of the heat flux in the cross section Z, removed from its surface, is determined by the expression

$$q_3(T_3, Z) = \bar{\alpha}_3(Z)\,(T_3 - T_{g1})\,. \tag{10}$$

As is shown in [7], the heat-transfer coefficient for the mixed-convection flow $\bar{\alpha}_3(Z)$ can be determined from the relation

$$\bar{\alpha}_3 = \bar{\alpha}_{3,N}\left[1 + \left(\bar{\alpha}_{3,F}/\bar{\alpha}_{3,N}\right)^3\right]^{1/3}. \tag{11}$$

In the case of free convection, the heat-transfer coefficient $\bar{\alpha}_{3,N}$ is determined according to (4); for the forced convection component $\bar{\alpha}_{3,F} = \mathrm{Nu}_{3,F}\lambda_g/l$ it is determined from the formula [8]

$$\mathrm{Nu}_F = 0.661\,\mathrm{Pr}^{0.33}\,\mathrm{Re}_l^{1/2}\,. \tag{12}$$

It is assumed that the width of the fin is small in comparison with the width of the cocurrent flow and the velocity of the cocurrent flow on the axial line can be used as U_x. Heat exchange on the surface of fin 5 and on the surface of fin 3 occurs in the cocurrent flow, has two components of the heat flux, and is calculated by the same method. The difference is that the cocurrent flow is formed in the case where there are two sources (fins 1 and 3) in it. These sources may be considered as a certain total heat source with a power $Q_1 + Q_3$ located on the line with a coordinate $x = x_3$. To calculate the dynamic and thermal characteristics of the cocurrent flow for the new efficient source, in expressions (6)–(8), instead of Q_1, we should write $Q_1 + Q_3$, where $Q_3(Z) = 2q_3(Z, T_3)l$ is the power of the second linear heat source (fin 3), and use the quantity $x = x_3$ instead of $x_1 = l/2$. Let us determine the value of the coordinate of formation of the heat source x_3. Assuming that the thickness of the boundary layer for the cocurrent flow from two sources is equal to the thickness of the boundary layer for the cocurrent flow from the lower source, from the condition $\delta_{g1}(x = 3l) = \delta_{g2}(x = 3l)$ we find the coordinate x_3:

$$x_3 = 3l - (1 + Q_3/Q_1)^{1/2}\,(3l - x_1)\,. \tag{13}$$

For the subsequent fins in one row ($i \ge 5$), the method of heat calculation of fins remains the same. In calculating the velocity and temperature of the flow on the axial line and of the thickness of the boundary layer for the cocurrent flow near the ith fin, formulas (6)–(8) take the form

$$U_{ix} = \left(\frac{2g\beta\,(Q_1 + Q_3 + \dots + Q_i)}{c_p I}\right)^{2/5} \left(\frac{x - x_i}{\mu\rho}\right)^{1/5} f'_{\mathrm{N}}(0)\,, \tag{14}$$

$$T_{gi} - T_{g\infty} = \left(\frac{(Q_1 + Q_3 + \dots + Q_i)^4}{64 g\beta\rho^2\mu^2 c_p^4 I^4}\right)^{1/5} (x - x_i)^{-3/5}\,, \tag{15}$$

$$\delta_{gi} = \left(\frac{16\mu c_p I\nu^2}{g\beta\,(Q_1 + Q_3 + \dots + Q_i)}\right)^{1/5} \eta_{\mathrm{e}}\,(x - x_i)^{2/5}\,, \quad i = 3, 5, 7, \dots\,, \tag{16}$$

where the power of the linear heat source for the ith fin is $Q_i = 2q_i l$; the density of the heat flux removed from the surface of the ith fin is determined by the expression

$$q_i\,(T_i, Z) = \bar{\alpha}_i\,(Z)\,(T_i - T_{\mathrm{g},i-1})\,, \tag{17}$$

and the coordinate of the total heat source x_i is found from the formula

$$x_i = il - \left(1 + \frac{Q_i}{Q_1 + Q_3 + \dots + Q_{i-2}}\right)^{1/2} (il - x_{i-2})\,, \quad i = 3, 5, 7, \dots\,. \tag{18}$$

For the fins of the neighboring row, the calculation of the thermal and dynamic characteristics of the cocurrent flow before the line of coalescence of the flows remains the same. Taking into account the fact that in the case of staggered arrangement of the fins, the neighboring rows are shifted by l, in expressions (3)–(18), instead of the coordinate x, we should use $x - l$, and the subscript i takes the values $i = 2, 4, 6, \dots$ instead of the values $i = 1, 3, 5, \dots$. The above-described method of calculation of heat transfer is used before the line of coalescence of the cocurrent flows. Taking into account the shift of the neighboring rows of fins, we determine the coordinate of the point of coalescence of the cocurrent flows x_{c}

$$\delta_{gm}\,(x_{\mathrm{c}}) + \delta_{gm}\,(x_{\mathrm{c}} - l) = s/2\,, \tag{19}$$

where the subscript m is the number of the fin, near which the cocurrent flows coalescence. It is assumed that after the coalescence of the boundary layers, the velocity and the temperature of the flow are equalized in the cross section between the rows of the fins, and in the calculations we use their average values and the flow is close to the developed flow in the channels, where the following equations of transfer of momentum and energy are true [9]:

$$\mu \frac{\partial^2 U}{\partial y^2} = -g\beta\rho\,(T_g - T_{g\infty}) + \frac{\partial p}{\partial x}\,, \tag{20}$$

$$\rho c_p U \frac{\partial T_g}{\partial x} = \lambda_g \frac{\partial^2 T_g}{\partial y^2}\,. \tag{21}$$

Let us integrate Eq. (20) over the channel width, taking into account the relations

$$\mu \left.\frac{\partial U}{\partial y}\right|_{y=0} = \tau\,(x)\,, \quad \left.\frac{\partial U}{\partial y}\right|_{y=s/2} = 0\,, \tag{22}$$

where the local shear friction stress on the fin surface for forced flow in the case of formation of a boundary layer on the fin surface is determined by the expression [10]

$$\tau\,(x) = \mu U \sqrt{\frac{U}{\nu x}}\, f_F''\,(0)\,, \tag{23}$$

and $f_F''(0)$ is the value of the second derivative of the self-similar variable $f_F(\eta)$ on the fin surface. Equation (20), when integrated with respect to the variable y, takes the form

$$\frac{\partial \bar{p}}{\partial x} = -\tau\,(x) + g\beta\rho\,(\bar{T}_g - T_{g\infty})\,. \tag{24}$$

Let us integrate Eq. (24) with respect to the coordinate x within the width of an individual fin and obtain the change in the pressure on this portion:

$$\Delta\bar{p}_i = -4 f_F''\,(0)\,\rho\nu^2\,(sl)^{-1}\,\mathrm{Re}_{il}^{3/2} + g\beta\rho\Delta\bar{T}_{gi}\,, \tag{25}$$

where $\Delta\bar{T}_{gi}$ is the change in the temperature of the external flow on the portion considered.

The averaged temperature of the heat-transfer agent in the channel $\bar{T}_{gi}$ is found upon integration of Eq. (21) over the channel width with allowance for the boundary conditions

$$\lambda_g \left.\frac{\partial T_{gi}}{\partial y}\right|_{y=0} = \bar{\alpha}_i\,(T_i - T_{gi})\,, \quad \left.\frac{\partial T_{gi}}{\partial y}\right|_{y=s/2} = 0\,. \tag{26}$$

Assuming that the temperature of the heat-transfer agent in the region of developed flow differs insignificantly from its average value, upon averaging we have

$$\rho c_p U_i \frac{\partial \bar{T}_{gi}}{\partial x} = \bar{\alpha}_i\,(T_i - \bar{T}_{gi})\,. \tag{27}$$

Upon integration of Eq. (27) in the direction $0x$ over the width of the ith fin on the assumption that U_i changes insignificantly on this portion we find

$$\bar{T}_{gi}\,(x = il) - T_i = (\bar{T}_{g,i-1}\,(x = (i-1)\,l) - T_i)\,\exp\left(-\frac{\bar{\alpha}_i l}{\rho c_p U_i}\right). \tag{28}$$

When the temperature of the external flow in the region of developed flow is determined, calculation is performed from the coordinate of coalescence of the cocurrent flows, and the temperature of the heat-transfer agent $\bar{T}_g(x = x_c)$ is averaged over the cross section of the cocurrent flows for the neighboring rows:

$$\bar{T}_g\,(x = x_c) = \frac{2}{s}\left[\int_0^{y_c} T_g\,(x = x_c, y)\,dy + \int_{y_c}^{s/2} T_g\,(x = x_c - l, y)\,dy\right], \tag{29}$$

where x_c, $y_c = \delta_{gc}$ are the coordinates of coalescence of the cocurrent flows. Upon passage to the variable η in the integrals of expression (29), using formula (15) and taking into account that at the point of coalescence of the cocurrent flows $\eta_e = \frac{y_c}{x_c}\sqrt[4]{\mathrm{Gr}_{x_c}/4}$ and $\eta_e = \frac{s/2 - y_c}{x_c - l}\sqrt[4]{\mathrm{Gr}_{x_c - l}/4}$, we determine the average temperature of the flow

$$\bar{T}_g\,(x = x_c) = T_{g\infty} + \frac{2R}{s}\left\{\left[\frac{\nu\,(Q_1 + Q_2 + ... + Q_{m-1})^3}{4g^2\beta^2\rho^3 c_p^3 I^3}\right]^{1/5}(x_c - x_{m-1})^{-1/5}\right.$$
$$\left.+\left[\frac{\nu\,(Q_2 + Q_4 + ... + Q_{m-2})^3}{4g^2\beta^2\rho^3 c_p^3 I^3}\right]^{1/5}(x_c - x_{m-1} - l)^{-1/5}\right\}, \tag{30}$$

where $R = \int_0^{\eta_e}\theta_g(\eta)d\eta$, that can be calculated with the use of the relation [6]

$$\int_0^{\eta_e}\theta_g\,(\eta)\,d\eta = \frac{16}{5}\int_0^{\eta_e} f_N'^2\,(\eta)\,d\eta\,.$$

Taking into account that the velocity of flow in the interfin channel changes from fin to fin, we determine its value near the ith fin. Assuming that the velocity, temperature, and pressure of the region of developed flow change insignificantly in the cross section of the channel and $U_i(x, y) \approx \bar{U}_i(x)$, $T_g(x, y) \approx \bar{T}_g(x)$, and $p(x, y) \approx \bar{p}(x)$, we integrate Eq. (20) with respect to the variable y and determine the velocity of the flow:

$$U_x = \frac{1}{2}\left[\frac{g\beta\rho}{\mu}\,(\bar{T}_g - T_{g\infty}) - \frac{1}{\mu}\frac{\partial\bar{p}}{\partial x}\right](sy - y^2)\,. \tag{31}$$

Upon averaging of the velocity over the channel width, we assume that $\partial\bar{p}_i/dx \approx \Delta\bar{p}_{il}/l$ on the portion equal to the width of the ith fin and find the change in the velocity on the portion:

$$\Delta\bar{U}_{ix} = \frac{1}{12}\left[\frac{\nu}{s}\,\mathrm{Gr}_s\,\frac{\Delta\bar{T}_{ig}}{T_0 - T_{g\infty}} - \frac{s^2}{\mu}\,\frac{\Delta\bar{p}_{il} - \Delta\bar{p}_{i-1,l}}{l}\right]. \tag{32}$$

The velocity in the region of developed flow is calculated from the point of joining of the cocurrent flows and its change on the portion $\Delta x = l$ for the ith fin is determined from formula (32). The initial value of the velocity in this region is found by averaging the velocity of the cocurrent flows at the point of coalescence of the boundary layer for the neighboring rows of fins:

$$\bar{U}_x\,(x = x_c) = \frac{2}{s}\left[\int_0^{y_c} U_x\,(x = x_c, y)\,dy + \int_{y_c}^{s/2} U_x\,(x = x_c - l, y)\,dy\right]. \tag{33}$$

As a result of the averaging, upon passage to the self-similar variable, using relation (14) we have

$$\bar{U}_x\,(x = x_c) = \frac{2J}{s}\left\{\left[\frac{4^3 g\beta\nu^2\,(Q_1 + Q_2 + ... + Q_{m-1})}{\rho c_p I}\right]^{1/5}(x_c - x_{m-1})^{3/5}\right.$$

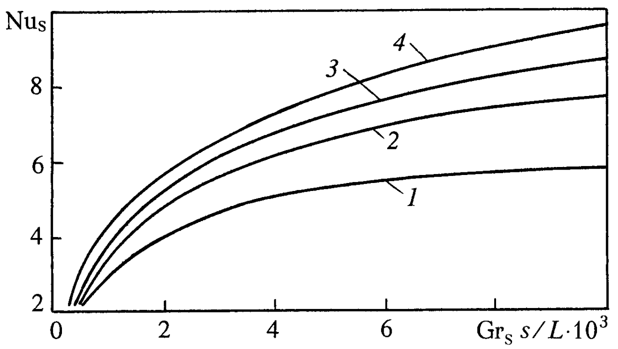

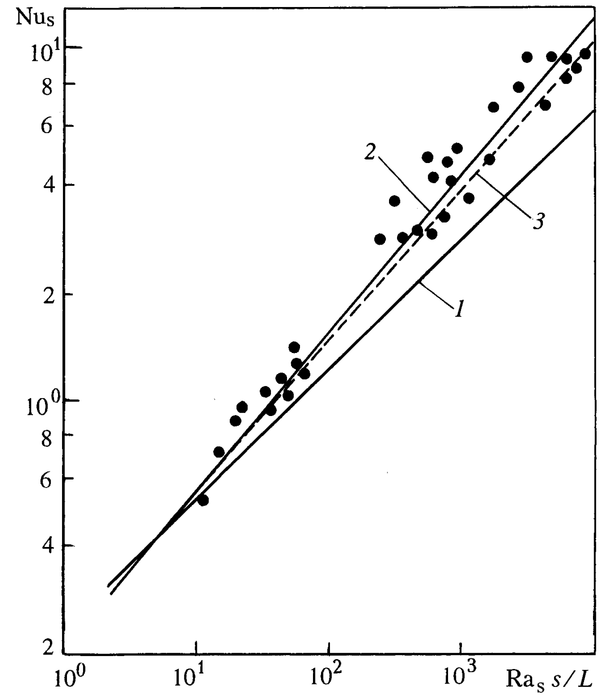

Fig. 3. Dependence of the Nu_s number on the parameter $Gr_s s/L$ for different numbers of fins in the adjacent rows: 1) surface with a continuous finning; 2) n = 10, 3) 25, and 4) 50.

Fig. 4. Comparison of the experimental and calculated values of the Nu_s number: 1) continuous finning [11]; 2) experimental data [3]; 3) calculated curve.

$$+\left[\frac{4^3 g\beta\nu^2 (Q_2 + Q_4 + ... + Q_{m-2})}{\rho c_p I}\right]^{1/5} (x_c - x_{m-1} - l)^{3/5}\Bigg\} , \tag{34}$$

where $J = f(\eta_e) \approx f(\infty)$ [6].

Since Eqs. (20) and (21) are interrelated, to refine the averaged values of the flow velocity and the temperature of the heat-transfer agent in the region of developed flow we organized the iteration procedure for calculating these values.

Thus, the problem of calculation of the heat exchange in the vertical surface with a discrete finning is reduced to the calculation of the velocity and temperature of the cocurrent flow in the interfin channel and the calculation of the heat transfer in individual fins according to Eq. (1). The densities of the heat flux q_i (i = 1, 2, ..., n) are determined by expressions (3), (10), and (17). The calculation is carried out in each zone from fin to fin, beginning with the first fin (Fig. 2). From Eq. (1) we determine the temperature characteristics of the fin. Then, we find the dynamic and thermal characteristics of the cocurrent flow by the above-described method and use them to calculate the temperature of the second fin, and so on.

A numerical calculation of Eq. (1) with boundary conditions (2) was carried out with the use of the Runge–Kutta scheme [11]. Some results of the numerical calculation for the surface with discrete steel fins having dimensions $50 \times 5 \times 0.5$ mm are presented in Figs. 3–6. In particular, Fig. 3 shows the dependences of the number $Nu_s = \overline{\alpha}s/\lambda_g$ on the parameter $Gr_s s/L$ for the surfaces with a discrete finning for different numbers of fins n in the adjacent rows along the height of the finned system. An analysis of the dependences obtained shows that, increasing the number of fins (or decreasing their length l), one can intensify the process of heat exchange of the surfaces considered. As follows from Fig. 3, an increase in the interfin space s and a decrease in the vertical dimensions of the base L leads to an increase in Nu_s. The quantitative estimates of the intensification process for discrete fins, made for the number of fins n = 25 and the values of the parameter $Gr_s s/L \sim 10^4$, show that, in comparison with continuous plates, the use

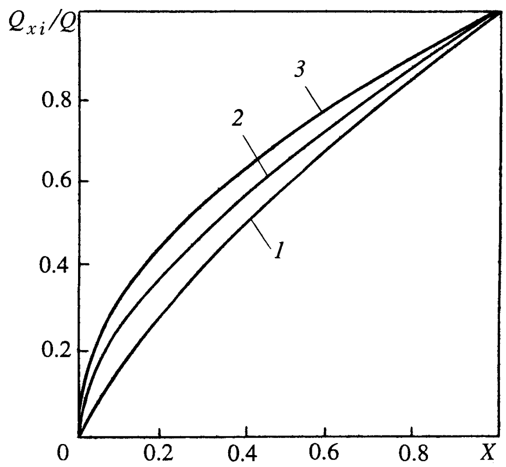

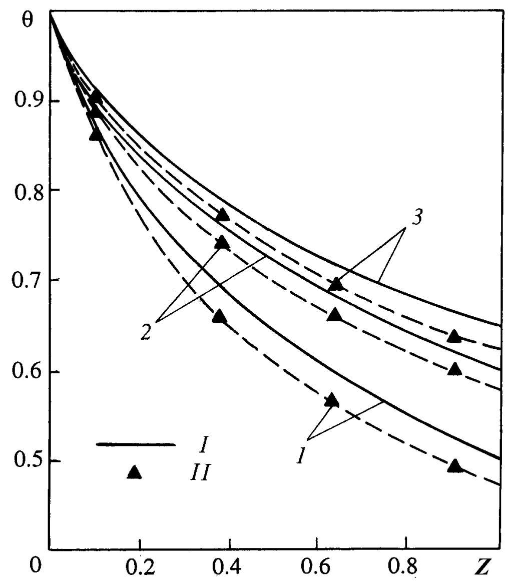

Fig. 5. Dependence of the quantity Q_{xi}/Q on the longitudinal coordinate X for the surface with a discrete finning: 1) n = 10, 2) 25, and 3) 50.

Fig. 6. Temperature distributions in the fins located on different portions of the base (I) calculation, II) experiment [3]): 1) i = 1, 2) 25, and 3) 49.

of discrete fins makes it possible to increase Nu_s by approximately 40%. An increase in the number of fins to n = 50 leads to an increase of 68% in Nu_s. It is of interest to compare the results obtained with the available data of the theoretical calculations for the analogous system of discrete fins with a constant temperature of the surface [4]. As follows from the comparative analysis, neglect of the real distribution of the temperatures along the fin height leads to errors toward overstating the degree of intensification. For example, according to [4], at n = 50 and $\mathrm{Gr}_s s/L \sim 10^4$ the total heat flux removed from the surface increases by approximately 90% in comparison with a continuous finning, which exceeds the values obtained in the present investigations by more than 20%.

Figure 4 shows the calculated and experimental data for the Nu_s numbers [3] obtained for the surface with steel fins with dimensions 50 × 11 × 1 mm for different numbers of fins in the neighboring rows along the height of the system. As follows from the figure, the calculated and experimental data are in satisfactory agreement. The maximum calculation error does not exceed 10–15%. Figure 4 also shows the experimental dependence [12] for vertical surfaces with a steel continuous finning. As follows from the comparison, the maximum intensification that is attained by discretization of the finning is 50–70%.

It is of importance to determine in what regions of the finned surface the heat removal is maximum and to make comparative estimates of the removed heat flux along the height of the system. Figure 5 shows the dependences Q_{xi}/Q, where $Q_{xi} = \sum_{j=0}^{i} \int_0^h \bar{\alpha}_j (T_j - \bar{T}_{gj}) dz$ is the heat flux removed from the region of the vertical surface of length $x_i = il$ and $Q = \sum_{i=1}^{n} \int_0^h \bar{\alpha}_i (T_i - \bar{T}_{gi}) dz$ is the total heat flux removed from the surface. The main heat removal occurs in the lower region of the radiator. For example, at n = 25, about 40% of the entire removed heat flux is removed from the surface of length $0 \le x/L \le 0.2$, which is a fifth of the total surface, and 75% of Q is removed from the surface $0 \le x/L \le 0.5$, i.e., from half of the total heat-exchange surface. For n = 50, these values are even higher. Consequently, in designing such surfaces it makes sense to decrease the vertical dimensions of the finned system.

Figure 6 shows results of the comparison of the calculated and experimental data [3] for the temperature distributions along the height of the steel fins with dimensions 50 × 11 × 1 mm on different portions along the height of the vertical base of length L = 500 mm with a staggered arrangement of the discrete finning. The largest decrease in the temperature head is observed for the lower fins and the smallest decrease is observed for the fins in the upper region of the finned surface. The difference between the calculated and experimental distributions does not exceed 15%.

NOTATION

x, y, z, running coordinates; T, temperature; q, density of the removed heat flux; p, pressure; h, height of the fin; l, width of the fin; L, vertical dimension of the finned surface; s, interfin distance; U, velocity of flow; g, free-fall acceleration; Q, total heat flux or power of the heat source; δ, thickness; ρ, density of the external heat-transfer agent; λ, thermal-conductivity coefficient; α, local heat-transfer coefficient; $\overline{\alpha}$, mean heat-transfer coefficient; μ, kinematic coefficient of viscosity; ν, dynamic viscosity; η, self-similar variable and efficiency of the fin; β, coefficient of volumetric expansion; τ, local shear friction stress; c_p, specific heat capacity; n, number of fins in the adjacent rows; $X = x/L$, $Z = z/h$, dimensionless coordinates; $\theta = (T - T_{g\infty})/(T_0 - T_{g\infty})$, dimensionless temperature; $\mathrm{Bi} = \alpha\delta/\lambda$, Biot number; Nu, Nusselt number; $\mathrm{Gr}_x = g\beta(T - T_{g\infty})x^3/\nu^2$, Grashof number; Pr, Prandtl number; $\mathrm{Re}_x = Ux/\nu$, Reynolds number; $\overline{T}_g = \frac{2}{s}\int_0^{s/2} T_g dy$, $\overline{U} = \frac{2}{s}\int_0^{s/2} U dy$, and $\overline{p} = \frac{2}{s}\int_0^{s/2} p dy$, temperature, velocity, and pressure of the flow averaged over the cross section. Subscripts: N, free (natural) convection; F, forced convection; f, fin; 0, base of the fin; ∞, environment; g, external heat-transfer agent; s, surface; e, boundary of the boundary layer; c, coalescence of cocurrent flows.

REFERENCES

1. V. G. Gorobets and V. V. Treputnev, in: *Proc. Int. School-Seminar "Problems of Heat and Mass Transfer in Processes and Apparatuses in Utilization of Secondary Energy Resources and Alternative Energy Sources"* [in Russian], Minsk (1990), pp. 136–142.
2. V. V. Treputnev and V. G. Gorobets, in: *Proc. II Minsk Int. Forum "Heat and Mass Transfer-92"* [in Russian], Vol. 1, Pt. 1, Minsk (1992), pp. 154–158.
3. V. G. Gorobets and V. V. Treputnev, *Prom. Teplotekh.*, No. 1, 55–60 (1999).
4. E. M. Sparrow and S. Prakash, *Heat Transfer* [Russian translation], No. 2, 34–41 (1980).
5. Y. Jaluria, *Natural Convection Heat and Mass Transfer* [Russian translation], Moscow (1983).
6. B. Gebhart, I. Pera, and A. W. Schorr, *Int. J. Heat Mass Transfer*, **13**, No. 1, 161–171 (1970).
7. I. Shai and Y. Barnea, *Int. J. Heat Mass Transfer*, **29**, No. 8, 1139–1147 (1986).
8. T. Cebeci and P. Bradshaw, *Physical and Computational Aspects of Convective Heat Transfer* [Russian translation], Moscow (1987).
9. L. N. Tao, *J. Heat Transfer*, **82**, No. 3, 233–238 (1960).
10. H. Schlichting, *Boundary Layer Theory* [Russian translation], Moscow (1974).
11. N. N. Kalitkin, *Numerical Methods* [in Russian], Moscow (1973).
12. V. V. Treputnev and V. G. Gorobets, *Prom. Teplotekh.*, No. 6, 19–24 (1998).